Am J Transl Res 2017;9(6):3017-3026
www.ajtr.org /ISSN:1943-8141/AJTR0047208

Original Article

Sapylin promotes wound healing in mouse skin flaps

Huijing Huang[1], Deguang Kong[2], Yu Liu[1], Qiuxia Cui[3], Kun Wang[3], Dan Zhang[3], Jinli Wang[1], Maocai Zhai[1], Jinhua Yan[1], Cuntai Zhang[1], Gaosong Wu[2]

Departments of [1]Geriatrics, [3]Thyroid and Breast Surgery, Tongji Hospital of Tongji Medical College, Huazhong University of Science and Technology, Wuhan 430030, P. R. China; [2]Department of Thyroid and Breast Surgery, Zhongnan Hospital of Wuhan University, 169 Dong Hu Road, Wuhan 430071, P. R. China

Received December 23, 2016; Accepted April 19, 2017; Epub June 15, 2017; Published June 30, 2017

Abstract: Seroma formation is one of the most common complications after modified radical mastectomy. Sapylin is an agent used to reduce seroma formation following breast cancer surgery. In this article, we aimed to identify the potential mechanism by which Sapylin reduced seroma formation. Thirty-six female C57 mice were randomly divided into three groups. All mice were anaesthetized and a skin flap was generated on their abdomens. Each group was treated with normal saline, 0.5 KE/ml of Sapylin, or 50% hypertonic glucose, respectively. On day 3 and day 7 after the surgery, six mice in each group were sacrificed. Skin flap samples were collected and markers of angiogenesis, collagen synthesis, fibroplasia and matrix remodeling were detected. The skin flaps from the Sapylin- or hypertonic glucose-treated mice closed faster than the skin flaps from the mice treated with normal saline. The neovessel density was higher in the skin flaps from the mice in the Sapylin group than those in the other two groups. Increased mRNA and protein expression of angiogenesis markers (VEGF-A and HIF-1α) and collagen synthesis markers (FGF2 and TGF-β1) were observed in the mice in the Sapylin group compared with the saline- or hypertonic glucose-treated mice. The extracellular matrix remodeling marker MMP2 was induced by Sapylin only in the early phase (day 3). In conclusion, Sapylin accelerated wound closure, and promoted angiogenesis, collagen synthesis and the remodeling process, which improved wound healing. Considering the close relationship between wound healing and seroma formation, Sapylin may reduce seroma formation after modified radical mastectomy.

Keywords: Sapylin, seroma formation, wound healing, modified radical mastectomy, breast cancer

Introduction

Breast cancer is the most frequently diagnosed cancer and accounts for approximately a quarter of the total number of new cancer cases in females [1]. Modified radical mastectomy is still the most common surgical treatment for breast cancer; however, seroma formation is a frequent complication of this procedure, particularly when axillary dissection is performed. Seromas increase the risks of skin flaps necrosis or infection, which affects the postoperative chemotherapy, radiation therapy, and other comprehensive treatments [2]. Seroma formation is known to have a strong connection with wound healing. Seroma accumulation elevates the flaps from the chest wall and axilla, which hampers their adherence to the tissue bed and delays the wound healing process [3]. In contrast, impaired wound healing, particularly areas containing damaged lymphatic vessels with increased lymph leakage, significantly contributes to the seroma volume [4]. Ideal wound healing minimizes lymph leakage and serum oozing, which allows the skin flaps to securely adhere to chest wall structures, obliterates the "dead space", and allows fluid to be rapidly removed as it forms. A study from Dr. Harper's group showed that autologous platelet-leukocyte-enriched plasma, a prepared autologous blood product used in orthopedic surgery to promote wound healing, reduced the burden of postoperative drains and the incidence of seroma formation after latissimus dorsi breast reconstruction [5], indicating that the application of specific agents may be an efficient method to reduce seroma formation and promote wound healing.

Sapylin, also known as OK-432, is a mixture of freeze-dried avirulent group A *Streptococcus pyogenes* and penicillin G. OK-432 not only

reduced the suction drainage duration but also significantly reduced seroma formation and the need for aspiration punctures after modified radical mastectomy in our previous study [6]. In addition, Fasching reported that OK-432 reduced seroma formation by promoting wound healing [7]. However, the precise mechanism underlying the effects of Sapylin on seroma formation has not been elucidated. In this article, we sought to determine the mechanism by which Sapylin promotes wound healing and subsequently reduces postoperative seroma formation and to provide additional evidence for the use of Sapylin on patients who experienced surgical trauma in the clinic.

Materials and methods

Animals

This prospective, controlled, experimental study was conducted using 36 adult female C57 mice, weighing 16-18 g (average =17 g). The study protocol was approved by the Ethics Committee for Animal Experiments of Tongji Hospital. All animals were maintained under the Specific Pathogen-Free (SPF) conditions with a 12-h light/dark cycle, a temperature of 24°C, and food and water available *ad libitum* at Laboratory Animal Center, Huazhong University of Science and Technology.

Wound model

The thirty-six mice were randomly divided into three groups of twelve: normal saline-treated (NS), 50% hypertonic glucose-treated (HG), and Sapylin-treated (SA) mice. Normal saline was used as a placebo and 50% hypertonic glucose, which is a classical agent used to promote wound healing in the clinic [8], served as a positive control. The same surgeon performed the same procedure on all mice in a sterile operating room. All the mice were anaesthetized with an intraperitoneal injection of 0.1 ml/10 g of 3.5% chloral hydrate. The abdominal hair of each mouse was shaved and depilated using a depilatory cream. A 6-7 mm incision was made in the abdominal dermis, which was then bluntly dissected using bent vessel forceps to form a skin flap. We next infused 50 μl of normal saline, 50% hypertonic glucose or 0.5 KE/ml Sapylin into the subcutaneous pocket of the NS, HG or SA mice, respectively. Finally, the incisions were closed using continuous ophthalmological sutures.

Six animals in each group were sacrificed on the third and seventh days after the surgery using an overdose of 3% pentobarbital sodium. The skin flaps and tissues underlying the surgical region were excised. A portion of each specimen was cut and fixed in 4% paraformaldehyde, and the remaining tissue sample was snap frozen in liquid nitrogen and stored at -80°C until RNA and protein extraction. The histological evaluation was performed using hematoxylin and eosin (H&E) staining and immunohistochemical staining on multiple serial sections (4-5 μm). Masson's trichrome staining was used to evaluate the collagen content.

Immunohistochemical staining and scoring, vessels counting

The fixed specimens were embedded in paraffin and cut into 4-5 μm-thick sections. The slides were deparaffinized with 2 changes of xylene and then transferred to decreasing concentrations of ethanol (100%, 95%, 70% and 50%) for 5 min each. Endogenous peroxidase activity was blocked by incubating the sections in a 3% H_2O_2 solution in methanol. After 3 rinses in phosphate buffer saline (PBS), the antigens were retrieved to unmask the antigenic epitope by incubating the slides in 10 mM citrate buffer, pH 6.0, at 95-100°C for 10 min. After cooling, 100 μl of 10% fetal goat serum was added to the sections to block non-specific antigen binding. The sections were then incubated with CD31 (1:100 dilution, Santa Cruz, CA) or HIF-1α (1:150 dilution, Santa Cruz, CA) antibodies in a humidified chamber at 4°C overnight. We then added 100 μl of an appropriately diluted biotinylated secondary antibody and incubated the sections at room temperature for 30 min. The sections were incubated in the streptavidin-biotin complex (BOSTER, China) for 20 min, followed by the diaminobenzidine (DAB) substrate solution until the desired color intensity was achieved. The slides were counterstained by immersion in hematoxylin for 1 min and then dehydrated using 4 alcohol solutions (95%, 95%, 100% and 100%). Finally, the slides were cleared using 3 xylene washes and then cover slipped using a mounting solution for permanent storage. Scores were calculated on intensity and percentage of positive staining cell nuclei (HIF-1α) in the whole tissue stains according to the article we previously published [9].

Neovessel density was assessed by light microscope (Olympus BX41, Japan) in areas containing the highest numbers of capillaries per area (neovascular "hotspots") [10]. Areas of highest neovascularization were found by scanning the sections at low magnification (×40 and ×100) and identifying those areas having the greatest numbers of distinct CD31 staining. Individual neovessels were counted on a ×400 field. Any brown-staining endothelial cell or endothelial cell cluster, clearly separate from adjacent microvessels and other connective-tissue elements, was considered a single, countable neovessel. Results were expressed as the highest number of neovessels identified within any single ×400 field.

Masson's trichrome staining

The sections were counterstained in Harris' hematoxylin for 5-10 min and then rinsed in water to remove the excess stain. The sections were incubated in 1% hydrochloric acid alcohol for 5 min and then washed in water and stained with 1% Ponceau S Red for 5 min. The sections were serially stained with 1% phosphomolybdic acid for 5 min, 2.5% aniline blue for 5 min, and 1% glacial acetic for 1 min and were then dehydrated in 95% and absolute alcohol. The sections were cleared in xylene. Finally, the slides were mounted in neutral balsam. The sections were photographed using a light microscope (Olympus BX41, Japan) and the images were analyzed using Image-Pro Plus software (National Institutes of Health).

Real-time PCR

Total RNA was isolated from the animal tissue samples using Trizol reagent according to the manufacturer's protocol. The total RNA was reverse-transcribed into cDNA using a reverse transcription kit (TOYOBO, Japan), followed by quantitative PCR to detect the expression levels of the VEGF-A, FGF2, HIF-1α and TGF-β1 mRNAs. GAPDH was used as an internal control. The thermal cycling conditions were as follows: 1 min at 95°C to activate the Taq DNA polymerase, followed by 40 cycles of amplification at 95°C for 15 s, 60°C for 15 s, and 72°C for 45 s. The reactions were performed in duplicate. The specific oligos used in the real-time PCR were as follows: VEGF-A (forward): 5'-ACGAACGTACTTGCAGATGTGA-3', VEGF-A (reverse): 5'-CTTTCCGGTGAGAGGTCTGG-3', HIF-1α (forward): 5'-ACCTTCATCGGAAACTCCAAAG-3', HIF-1α (reverse): 5'-CTGTTAGGCTGGGAAAAGTTAGG-3', TGF-β1 (forward): 5'-CTCCCGTGGCTTCTAGTGC-3', TGF-β1 (reverse): 5'-GCCTTAGTTTGGACAGGATCTG-3', FGF2 (forward): 5'-CGACCCACACGTCAAACTACA-3', FGF2 (reverse): 5'-GTAACACACTTAGAAGCCAGCA-3', GAPDH (forward): 5'-AGGTCGGTGTGAACGGATTTG-3', and GAPDH (reverse): 5'-TGTAGACCATGTAGTTGAGGTCA-3'. The gene expression values were calculated using the $2^{-\Delta\Delta CT}$ relative expression method.

Western blot analysis

Approximately 30 mg of frozen tissue were obtained from each animal and then ground in liquid nitrogen. Tissue lysates were extracted using ice-cold RIPA buffer and measured using a bicinchoninic acid (BCA) protein assay kit. Tissue extracts were fractionated on 10% sodium dodecyl sulfate-polyacrylamide gels using electrophoresis and then transferred to polyvinylidene fluoride membranes for 90 min at 300 mA. The membranes were subsequently blocked with 5% nonfat dry milk for 1 h at room temperature and then incubated with primary antibodies against mouse VEGF-A (1:1000 dilution, Santa Cruz, CA), FGF2 (1:1000 dilution, Santa Cruz, CA), HIF-1α (1:1000 dilution, Santa Cruz, CA), rabbit TGF-β1 (1:1000 dilution, Cell Signaling Technology, USA), MMP2 (1:1000 dilution, Cell Signaling Technology, USA) or β-Tubulin (1:1000 dilution, Cell Signaling Technology, USA) overnight at 4°C. The membranes were subsequently incubated with horseradish peroxidase-conjugated anti-mouse or anti-rabbit secondary antibody (1:5000 dilution, Cell Signaling Technology, USA) for 1 h at room temperature. Protein bands were visualized using enhanced chemiluminescence (Kodak Image Station 4000 MM Pro, USA). The band intensity was quantified using Image J software (National Institutes of Health).

Statistical analysis

All of the experimental data were statistically processed using SPSS 19.0 software (SPSS Inc., USA). The data for each study parameter from each group are presented as the mean ± SD. Differences were analyzed using an unpaired Student's t-test. P values <0.05 were considered statistically significant.

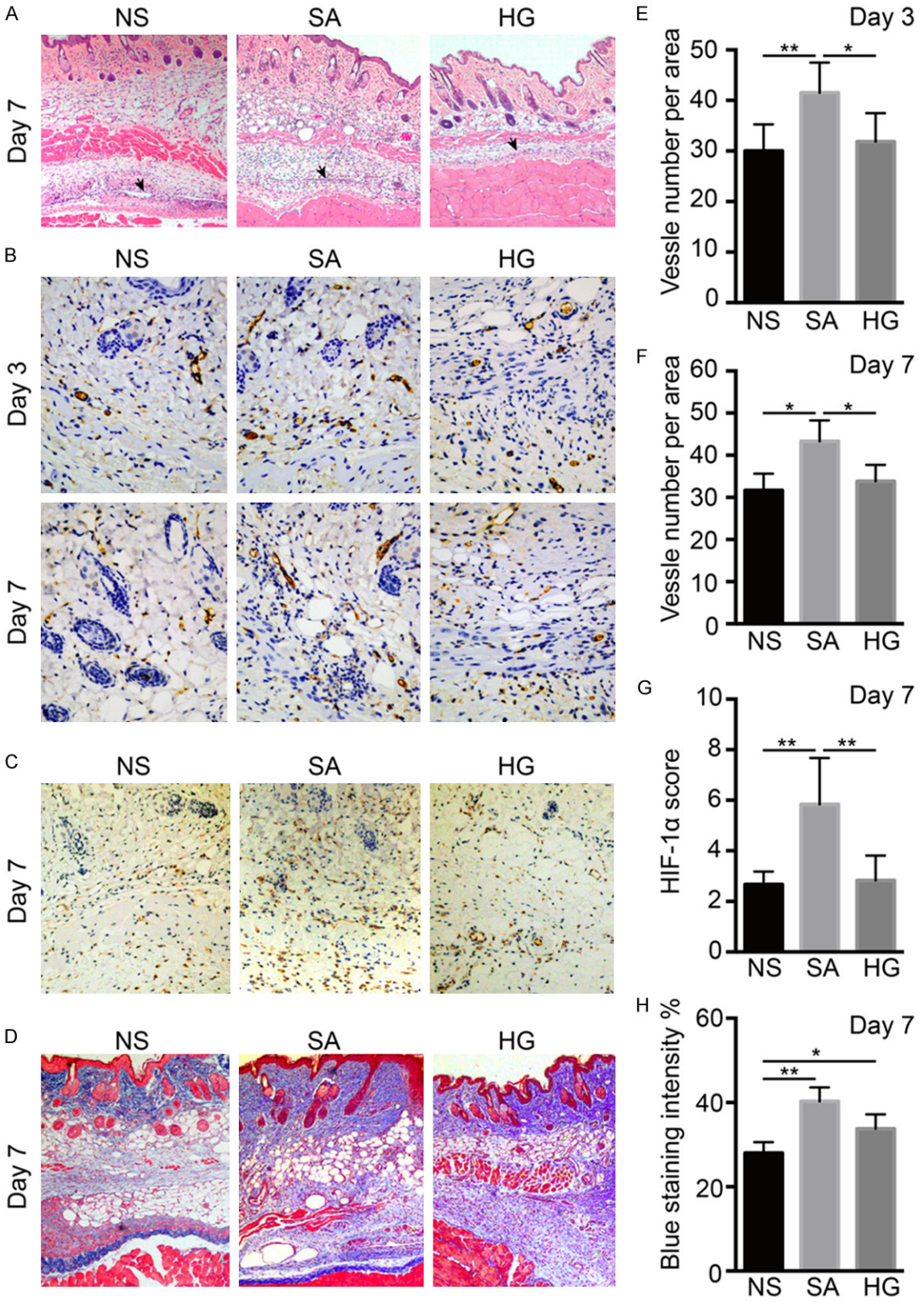

Figure 1. Sapylin promotes skin flaps closure, induces angiogenesis and collagen synthesis in the wound. A: The arrows show the unclosed space in the skin flaps in each group of mice. Sapylin and hypertonic glucose promote skin flaps closure compared with normal saline; B, E and F: The positive staining of CD31 represents the neovessels in the tissue. On day 3 and day 7, CD31 expression was higher in the SA group than the NS and HG group; C and G: HIF-1α-positive staining was increased in the SA group compared with the NS or HG groups on day 7; D and H: Masson's

trichrome staining in three groups of mice on day 7. The intensity of the blue staining was significantly increased in the skin flaps of the Sapylin- and hypertonic-treated mice compared with the NS mice. n=4, *P<0.05, **P<0.01.

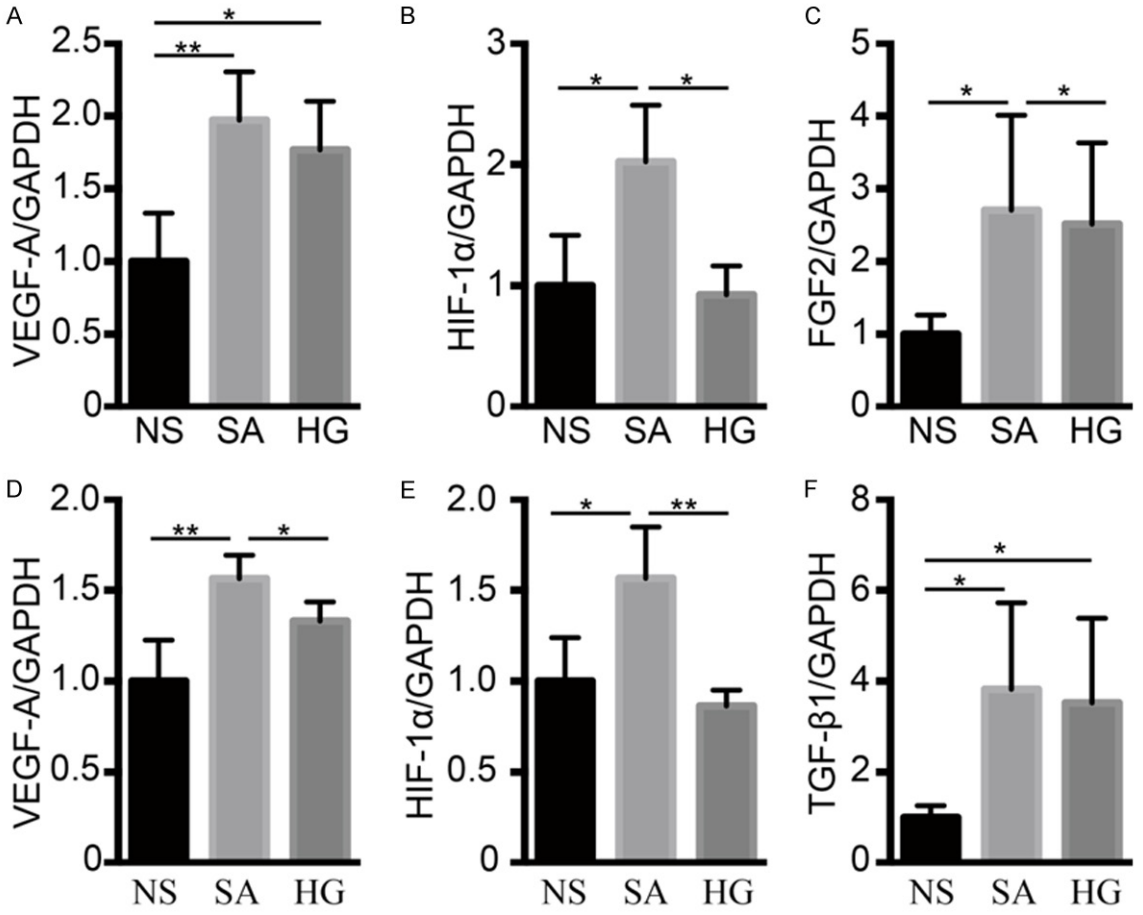

Figure 2. Sapylin promotes mRNA expression of markers related to wound healing. A-C: On day 3, the Sapylin treatment significantly upregulated VEGF-A, HIF-1α and FGF2 expression compared to the saline or hypertonic glucose treatments; D-F: On day 7, the Sapylin-treated tissue expressed higher levels of VEGF-A, HIF-1α and TGF-β1 than saline or hypertonic glucose-treated tissue. n=4, *P<0.05, **P<0.01.

Results

Sapylin promotes skin flap closure

As shown in the hematoxylin- and eosin-stained images in **Figure 1A**, seven days after the surgery, the Sapylin- and hypertonic glucose-treated skin flaps were completely closed, whereas there was a relatively large space in the skin flaps from the saline-treated group. By promoting skin flap closure, Sapylin decreased the opportunity for the seroma to remain in the "dead space".

Sapylin induces angiogenesis in mouse skin flaps

Because angiogenesis is an essential step of the wound healing process, we investigated whether Sapylin could induce angiogenesis in the skin flaps. For this purpose, we used immunohistochemical staining, real-time PCR and western blotting to identify the neovessels and molecular markers of angiogenesis in our samples. CD31 is a specific marker of vascular endothelial cells. As shown in **Figure 1B**, there was a significant increase in the density of CD31-positive cells in the skin flaps of the Sapylin-treated mice on days 3 or 7 after surgery compared to the other two groups. As shown in **Figure 2A**, on day 3, the Sapylin- and 50% hypertonic glucose-treated skin flaps showed higher VEGF-A mRNA levels than the normal saline-treated group (P<0.01 for SA versus NS, P<0.05 for HG versus NS). The expression of the VEGF-A protein indicated similar results (P<0.05 for SA or HG versus NS, **Figure**

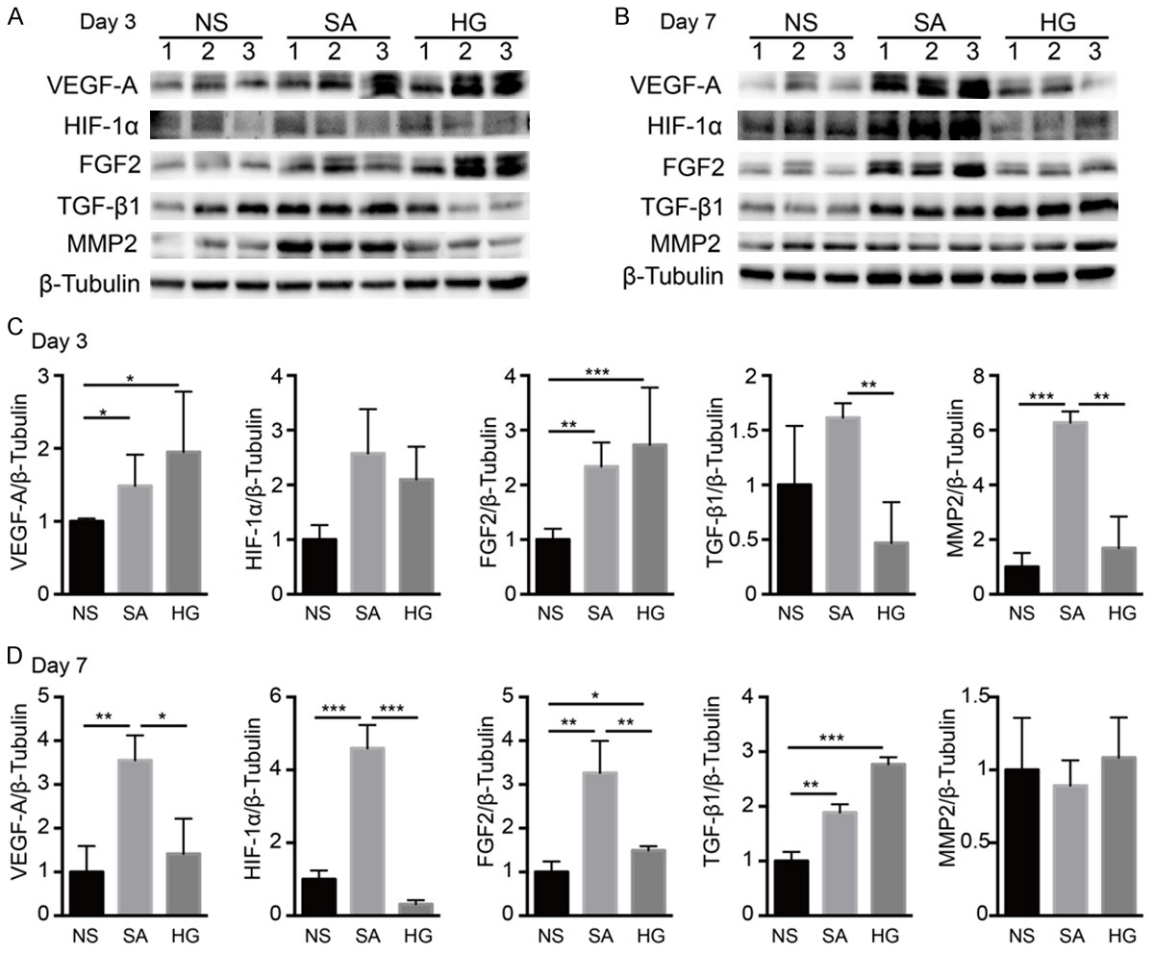

Figure 3. Sapylin promotes protein expression of wound healing markers. A and C: On day 3, angiogenesis marker VEGF-A and fibroplasia related proteins FGF2 and TGF-β1 were upregulated in the skin flaps of SA group mice. Only Sapylin induced MMP2 expression on day 3; B and D: On day 7, the expression of VEGF-A, HIF-1α, FGF-2 and TGF-1β was significantly upregulated by Sapylin. There were no differences in MMP2 expression among the three groups on day 7. n=3, *P<0.05, **P<0.01, ***P<0.001.

3A). The expression of the HIF-1α mRNA was higher in Sapylin-treated skin flaps than normal saline- and hypertonic glucose-treated skin flaps on day 3 (P<0.05 for SA versus NS and HG, **Figure 2B**). As shown in **Figure 3B**, seven days after the surgery, the Sapylin-treated skin flaps showed a significantly increase in VEGF-A (P<0.01 for SA versus NS, P<0.05 for SA versus HG) and HIF-1α expression (P<0.001 for SA versus NS and HG) compared with the other two groups. The analysis of the VEGF-A and HIF-1α mRNAs and the HIF-1α scoring confirmed the results of the protein expression analysis (**Figures 2D**, **2E** and **1C**). Based on these results, we can conclude that Sapylin induces angiogenesis in the skin flaps of our mouse model.

Sapylin promotes fibroplasia and collagen synthesis in the wound

According to the Masson's trichrome staining shown in **Figure 1D**, the intensity of the blue staining in the Sapylin- and hypertonic glucose-treated skin flaps was obviously higher than the normal saline-treated group on day 7. The intensity of the blue staining corresponds to the relative quantity of collagen fiber deposits, which reflects collagen synthesis, degradation, and remodeling in the tissue. Sapylin and hypertonic glucose efficiently promoted collagen synthesis in the mouse skin flaps (P<0.01 for SA versus NS and P<0.05 for HG versus NS). FGF2 is an important marker of fibroplasia and collagen synthesis. As shown in the western blot images in **Figure 3A**, the Sapylin and hyper-

tonic glucose treatments increased FGF2 expression on day 3 compared to the normal saline treatment (P<0.01 for SA versus NS, P<0.001 for HG versus NS), which was consistent with the mRNA levels among the three groups (P<0.05 for SA or HG versus NS, **Figure 2C**). On day 7, the skin flaps in the Sapylin-treated mice exhibited higher FGF2 expression than the skin flaps from the other two groups (P<0.01 for SA versus NS and HG, **Figure 3B**). TGF-β1 is known to have profound effects on the wound site, particularly through its influence on fibroblast migration and collagen deposition at the site of the scar. The Sapylin- and 50% hypertonic glucose-treated skin flaps produced more TGF-β1 than the normal saline-treated mice (P<0.01 for SA versus NS, P<0.001 for HG versus NS) on day 7 (**Figure 3B**). Additionally, as shown in **Figure 2F**, the levels of the TGF-β1 mRNA were also upregulated in the Sapylin- and hypertonic glucose-treated mice compared to the saline-treated mice (P<0.05 for SA or HG versus NS). In summary, Sapylin increased fibroplasia and collagen synthesis in the wound.

Sapylin induced MMP2 expression on day 3

As shown in the western blot image in **Figure 3A**, the extracellular matrix remodeling protein MMP2 was highly expressed only in the Sapylin-treated skin flaps on day 3 (P<0.001 for SA versus NS, P<0.01 for SA versus HG); however, there were no differences in MMP2 expression among the three groups on day 7, indicating that in the early phase of wound healing, Sapylin helped remove the damaged extracellular matrix and promoted angiogenesis and cell migration in the wounded tissue.

Discussion

Seroma formation is one of the most common complications after mastectomy and axillary lymph node dissection [11, 12]. Significant effort has been dedicated to prevent the occurrence of seromas. However, each approach has its limitations. In our study, skin flaps from Sapylin-treated mice showed accelerated wound closure and enhanced angiogenesis, collagen synthesis, fibroplasia and extracellular matrix remodeling, which are essential characteristics of wound healing, at both the molecular and histological levels compared to saline-treated and hypertonic glucose-treated mice. By promoting the wound healing process, Sapylin may reduce seroma formation in mouse skin flaps.

Sapylin was originally used as an immunotherapeutic agent to cure certain types of cancers [13], and it induces strong local T-cell reactions in the treated area [14]. To date, Sapylin has been used to reduce seroma formation after axillary lymphadenectomy to treat breast cancer and breast reconstruction surgery [15]. However, the mechanism underlying this function is still unclear. As reported in our previous study, Sapylin triggered the inflammatory cascade, which is why patients often suffer from a fever after an infusion of this drug [6]. Conversely, the inflammatory response also correlates to wound healing. Considering the significant relationship between wound healing and seroma formation, we hypothesized that Sapylin may reduce seroma formation by promoting wound healing. Therefore, we detected markers of wound healing in our samples.

Closed skin flaps adhere to the muscle layers, which removes the “dead space”, minimizes lymph spillage and serum oozing, and prevents seroma formation. According to the H&E staining in **Figure 1A**, on day 7, the Sapylin- and hypertonic glucose-treated skin flaps showed complete closure and adhered to the underlying tissue. Therefore, Sapylin accelerates the wound healing process and decreases the opportunity for the seroma to form in the skin flaps.

Angiogenesis occurs naturally during growth, reproduction, and wound healing to supply nutrients and oxygen to the tissues [16]. The early stages of angiogenesis begin with capillary formation and the initiation of sprouting into the wound bed by endothelial cell proliferation and migration in response to diverse cytokines and metabolic stimuli. The specific endothelial marker CD31 was upregulated in the Sapylin-treated group of mice compared to the other groups. We also observed a significant increase in the expression of molecular markers for angiogenesis (VEGF-A and HIF-1α) in the skin flaps of the Sapylin-treated group. VEGF-A is predominantly secreted by keratinocytes located in the wound periphery. Mechanical injury to the skin provokes a strong upregulation of VEGF-A expression, which temporally and spatially correlates with the proliferation of

new blood vessels [17]. VEGF-A expression during wound repair is thought to regulate different processes, including vascular permeability, the influx of inflammatory cells to the injury site, the migration and proliferation of pre-existing endothelial cells and the recruitment of marrow-derived endothelial progenitor cells to the local wound site, where they are able to accelerate repair [17-19]. As shown in **Figure 3A**, both the Sapylin and hypertonic glucose treatments promoted VEGF-A expression in the skin flaps on day 3. However, on day 7, VEGF-A expression was significantly increased in the Sapylin-treated group compared with the other two groups. Hypoxia-induced HIF-1α signaling influences a range of cell functions that play essential roles in various pathological or physiological processes, including angiogenesis, growth, and migration [20]. A loss of HIF-1α delays wound healing, reduces wound vascularity, and significantly impairs the ischemic neovascular response [21]. There was no difference in HIF-1α expression between the three groups on day 3. However, on day 7, only Sapylin induced a significant increase in HIF-1α expression.

Collagen and fibrin promote skin flap contraction and help free skin flaps adhere to the muscle, which accelerates iatrogenic lacuna closure and strengthens the incision. The Sapylin- and hypertonic glucose-treated skin flaps had a higher collagen content than the normal saline group. FGF2 and bFGF are released from macrophages and endothelial cells located in the wound and function as fibroplasia markers. These proteins stimulate the proliferation and migration of fibroblasts and keratinocytes, attract inflammatory cells and surrounding cells to the wound surface and induce various cytokines. Although the normal saline treatment did not increase FGF2 expression on day 3, the Sapylin and glucose treatments increased its expression. On day 7, FGF2 expression was significantly increased in the Sapylin-treated skin flaps compared with the saline- and hypertonic glucose-treated skin flaps. Additionally, the expression of TGF-β1, the crucial bioactive molecule in the wound healing process, was significantly increased in the skin flaps from the Sapylin- and hypertonic glucose-treated mice on day 7. TGF-β stimulates fibroplasia and collagen deposition and inhibits extracellular matrix degradation by upregulating the synthesis of protease inhibitors [22]. The administration of TGF-β1 into wound chambers or incisional wounds stimulates the accumulation of granulation tissue and the cellularization of the wound bed, which accelerates the wound healing process in experimental models [19, 23]. TGF-β1 also potently induces the expression of major extracellular matrix proteins, such as fibronectin and collagens [23], thus promoting extracellular matrix (ECM) deposition at the site of the wound healing.

As shown in **Figure 3A**, matrix metalloproteinase 2 (MMP2) was significantly expressed in the skin flaps of the Sapylin-treated on day 3 compared to the other two groups; however, no difference was observed between the groups on day 7. The principal function of MMPs is to degrade and remove the damaged ECM. MMPs also disrupt the capillary basement membrane to promote angiogenesis, cell migration, contraction and remodeling of the tissue [24]. However, excessive activation of specific MMPs was previously shown to impair cell migration and lead to the degradation of some necessary matrix proteins and growth factors [25]; overexpression of MMPs is thought to be responsible for the poor healing of chronic wounds [26]. Because Sapylin induced increased MMP2 expression among the three groups during the early phase of wound healing (day 3), it may promote angiogenesis and inflammatory cell migration in the skin flaps, indicating that Sapylin may improve wound healing in our animal model.

Our study has some limitations. Firstly, we used healthy mice in the study, which may not reflect the healing ability of women suffering from breast cancer. Secondly, the trauma from a modified radical mastectomy is much more severe than the wound created by our surgery. Therefore, further experimental and clinical studies are required to verify these results.

Conclusions

In summary, Sapylin is beneficial for wound healing by promoting wound closure and inducing angiogenesis, fibroplasia, collagen synthesis and matrix remodeling at the incision. By promoting wound healing through the mechanisms discussed above, Sapylin may partially reduce seroma formation after modified radical mastectomy. Therefore, we recommend Sapylin as an alternative choice for surgeons treating

seroma formation or delayed wound healing in the clinic.

Acknowledgements

This work was supported by the National Science Foundation of Hubei Province (No. 2012FFB02310) and China international medical foundation (Research projects of the thyroid gland disease undertook by young and middle-aged doctors in 2015, No. 2016026).

Disclosure of conflict of interest

None.

Address correspondence to: Dr. Gaosong Wu, Department of Thyroid and Breast Surgery, Zhongnan Hospital of Wuhan University, 169 Dong Hu Road, Wuhan 430071, P. R. China. Tel: 0086-138-7144-4606; E-mail: wugaosongtj@163.com; Dr. Cuntai Zhang, Department of Geriatrics, Tongji Hospital of Tongji Medical College, Huazhong University of Science and Technology, 1095 Jiefang Avenue, Wuhan 430030, P. R. China. Tel: 0086-159-2766-8408; E-mail: ctzhang@tjh.tjmu.edu.cn

References

[1] Torre LA, Bray F, Siegel RL, Ferlay J, Lortet-Tieulent J and Jemal A. Global cancer statistics, 2012. CA Cancer J Clin 2015; 65: 87-108.

[2] Tadych K and Donegan WL. Postmastectomy seromas and wound drainage. Surg Gynecol Obstet 1987; 165: 483-487.

[3] Agrawal A, Ayantunde AA and Cheung KL. Concepts of seroma formation and prevention in breast cancer surgery. ANZ J Surg 2006; 76: 1088-1095.

[4] Watt-Boolsen S, Nielsen VB, Jensen J and Bak S. Postmastectomy seroma. A study of the nature and origin of seroma after mastectomy. Dan Med Bull 1989; 36: 487-489.

[5] Harper JG, Elliott LF and Bergey P. The use of autologous platelet-leukocyte-enriched plasma to minimize drain burden and prevent seroma formation in latissimus dorsi breast reconstruction. Ann Plas Surg 2012; 68: 429-431.

[6] Kong D, Liu Y, Li Z, Cui Q, Wang K, Wu K and Wu G. OK-432 (Sapylin) reduces seroma formation after axillary lymphadenectomy in breast cancer. J Invest Surg 2017; 30: 1-5.

[7] Fasching G and Sinzig M. OK-432 as a sclerosing agent to treat wound-healing impairment. Eur J Pediatr Surg 2007; 17: 431-432.

[8] de Cabrera MA, Okamoto T and Cabrera-Peralta C. Influence of pre- and post-operative treatment with saline glucose solution on oral surgery wound healing. Histological study in rats. Rev Faculdade Odontol Lins 1988; 1: 4-11.

[9] Liu Y, Zhou R, Yuan X, Han N, Zhou S, Xu H, Guo M, Yu S, Zhang C, Yin T and Wu K. DACH1 is a novel predictive and prognostic biomarker in hepatocellular carcinoma as a negative regulator of Wnt/beta-catenin signaling. Oncotarget 2015; 6: 8621-8634.

[10] Weidner N, Carroll PR, Flax J, Blumenfeld W and Folkman J. Tumor angiogenesis correlates with metastasis in invasive prostate carcinoma. Am J Pathol 1993; 143: 401-409.

[11] Abe M, Iwase T, Takeuchi T, Murai H and Miura S. A randomized controlled trial on the prevention of seroma after partial or total mastectomy and axillary lymph node dissection. Breast Cancer 1998; 5: 67-69.

[12] Woodworth PA, McBoyle MF, Helmer SD and Beamer RL. Seroma formation after breast cancer surgery: incidence and predicting factors. Am Surg 2000; 66: 444-450.

[13] Oba MS, Teramukai S, Ohashi Y, Ogawa K, Maehara Y and Sakamoto J. The efficacy of adjuvant immunochemotherapy with OK-432 after curative resection of gastric cancer: an individual patient data meta-analysis of randomized controlled trials. Gastric Cancer 2016; 19: 616-624.

[14] Hovden AO, Karlsen M, Jonsson R, Aarstad HJ and Appel S. Maturation of monocyte derived dendritic cells with OK432 boosts IL-12p70 secretion and conveys strong T-cell responses. BMC Immunol 2011; 12: 2.

[15] Yang Y, Gao E, Liu X, Ye Z, Chen Y, Li Q, Qu J, Dai X, Wang O, Pan Y and Zhang X. Effectiveness of OK-432 (Sapylin) to reduce seroma formation after axillary lymphadenectomy for breast cancer. Ann Surg Oncol 2013; 20: 1500-1504.

[16] Re RN and Cook JL. An intracrine view of angiogenesis. Bioessays 2006; 28: 943-953.

[17] Brown LF, Yeo KT, Berse B, Yeo TK, Senger DR, Dvorak HF and van de Water L. Expression of vascular permeability factor (vascular endothelial growth factor) by epidermal keratinocytes during wound healing. J Exp Med 1992; 176: 1375-1379.

[18] Nissen NN, Polverini PJ, Koch AE, Volin MV, Gamelli RL and DiPietro LA. Vascular endothelial growth factor mediates angiogenic activity during the proliferative phase of wound healing. Am J Pathol 1998; 152: 1445-1452.

[19] Weis SM and Cheresh DA. Pathophysiological consequences of VEGF-induced vascular permeability. Nature 2005; 437: 497-504.

[20] Semenza GL. Oxygen sensing, hypoxia-inducible factors, and disease pathophysiology. Annu Rev Pathol 2014; 9: 47-71.

[21] Duscher D, Maan ZN, Whittam AJ, Sorkin M, Hu MS, Walmsley GG, Baker H, Fischer LH, Ja-

nuszyk M, Wong VW and Gurtner GC. Fibroblast-specific deletion of hypoxia inducible factor-1 critically impairs murine cutaneous neovascularization and wound healing. Plast Reconstr Surg 2015; 136: 1004-1013.

[22] Flanders KC and Burmester JK. Medical applications of transforming growth factor-beta. Clin Med Res 2003; 1: 13-20.

[23] Roberts AB, Sporn MB, Assoian RK, Smith JM, Roche NS, Wakefield LM, Heine UI, Liotta LA, Falanga V, Kehrl JH and Anthony SF. Transforming growth factor type beta: rapid induction of fibrosis and angiogenesis in vivo and stimulation of collagen formation in vitro. Proc Natl Acad Sci U S A 1986; 83: 4167-4171.

[24] Amato B, Coretti G, Compagna R, Amato M, Buffone G, Gigliotti D, Grande R, Serra R and de Franciscis S. Role of matrix metalloproteinases in non-healing venous ulcers. Int Wound J 2015; 12: 641-645.

[25] Signorelli SS, Malaponte G, Libra M, Di Pino L, Celotta G, Bevelacqua V, Petrina M, Nicotra GS, Indelicato M, Navolanic PM, Pennisi G and Mazzarino MC. Plasma levels and zymographic activities of matrix metalloproteinases 2 and 9 in type II diabetics with peripheral arterial disease. Vasc Med 2005; 10: 1-6.

[26] Martins VL, Caley M and O'Toole EA. Matrix metalloproteinases and epidermal wound repair. Cell Tissue Res 2013; 351: 255-268.